Desalination and Water Treatment
www.deswater.com

doi: 10.5004/dwt.2018.21500

136 (2018) 1–6
December

Effect of the tube surface temperature on the seawater fouling process during falling film evaporation outside horizontal tubes

Xiaohua Liu, Shuangyang Liu, Shubo Sun, Shengqiang Shen*, Peijie Mi

Key Laboratory of Ocean Energy Utilization and Energy Conservation of Ministry of Education, Dalian University of Technology, Dalian 116024, China, emails: zzbshen@dlut.edu.cn (S. Shen), lxh723@dlut.edu.cn (X. Liu), 190234758@qq.com (S. Liu), 1910760558@qq.com (S. Sun), 252452936@qq.com (P. Mi)

Received 27 May 2016; Accepted 15 October 2018

ABSTRACT

The technology of falling film evaporation outside horizontal tubes has been widely used in thermal desalination plants with advantages of the high heat transfer coefficient and low heat consumption. The seawater fouling during falling film evaporation outside horizontal tubes limits the increment of the top brine temperature and seriously reduces the heat transfer coefficient. This paper presents an experimental study of the heat transfer surface temperature effect on the seawater fouling process during falling film evaporation. Dalian local seawater is selected as the working agent. The scale growing curves under different conditions are obtained by weighting the scale mass at different time during fouling. The morphology and composition of scale layer are analyzed through a scanning electron microscopy and an energy dispersive X-ray spectroscopy. The results show that there exists no significant fouling process for the tube surface temperatures of 50°C and 53°C, but for the tube surface temperature over 53°C, the scale asymptotic *value* increases significantly. The tube surface temperature plays an important role on the content of Ca and Mg in scale layer. The content of Mg is greater than that of Ca for the tube surface temperature of 70°C, but it is opposite for the tube surface temperatures of 50°C and 60°C. The content of Mg increases with the tube surface temperature. For the tube surface temperature of 70°C, the content of Ca is smaller than that for the tube surface temperatures of 50°C and 60°C.

Keywords: Seawater desalination; Falling film evaporation; Fouling process; Tube surface temperature

1. Introduction

The shortage of freshwater in China is a serious problem. Seawater desalination technology can help to increase the total amount of freshwater, which provides a good solution to the shortage of freshwater. With unique advantages, low temperature multieffect evaporation seawater desalination technology has developed rapidly. Fouling on the outside surfaces of tubes in falling film evaporators is a key factor which reduces the heat transfer efficiency and limits the increase of the top brine temperature.

Scholars performed a lot of researches on fouling process. These studies focused on various properties, such as material, temperature, spray density and ion concentration [1]. Kern and Seaton [2] first presented the concept of net fouling rate which was the difference between deposition and removal rate in 1959. Kern–Seaton model for particle fouling was proposed. A turbulent model with non-equilibrium wall functions was used in a 3D numerical simulation to get the Nusselt number and wall shear stress, and the Von-Karman analogy was used to get the mass transfer coefficient [3]. Xu et al. [4] investigated the particulate fouling removal mechanism, explained the formation of induction step, redefined the initiation of fouling, and developed a predictive model by means of the turbulent burst theory [5]. Chan and Ghassemi [6] proposed a multispecies transport model to predict the calcium carbonate deposition. An ion diffusion model was proposed by the combining deposition process of Hasson et al. [7] with transfer theory. Wang et al. [8] developed a predictive model of $CaCO_3$ scaling rate.

* Corresponding author.

Many experiments on scale formation were also carried out. The fouling periods of $CaCO_3$ on cooper, aluminum, stainless steel and aluminum plating steel under different conditions were tested and compared. The results showed that the material, concentration, temperature and velocity were primary factors on the fouling period [9]. During the experimental study of crystallization fouling, Zhao [10] mainly focused on the effect of different external conditions on the scale formation, types and properties by using an X-ray diffraction, and a scanning electron microscopy (SEM). In addition to the tube surface temperature and material, Liu [11] systematically discussed the effects of surface roughness, modification, free energy and corrosion on the formation and adhesion of the calcium carbonate crystalline on metallic heat transfer surfaces.

In the actual operation of heat exchange equipment, the length of scale induction period is very significant. By distinguishing the induction period of scaling (IPS) and crystallization, a mathematical model was established for IPS of $CaCO_3$ which heterogeneously nucleated on heated surfaces [12]. The relationships between IPS and surface super saturation, surface temperature, flow velocity and other surface properties were obtained through computation. The fouling induction period of $CaCO_3$ was studied through micro video technology by Liu and Wang [13]. The rates of nucleating and nuclei growing were measured under various conditions. $CaCO_3$ fouling behaviors in both recirculated cooling water and pool boiling systems were studied by Yang et al. [14], in which the fouling morphology was analyzed through an SEM and an atomic force microscopy. The fouling characteristics in cooling water system, as well as the removal of scale, for both induction and post-induction periods, were investigated. Qiu et al. [15] gained the fouling induction periods in three kinds of heat exchangers made of stainless-steel, titanium and copper through experiment, and studied the effect of surface energy on fouling induction period by theoretical analysis. Li et al. [16] analyzed the effect of some parameters, such as saturation, temperature, flow velocity, the existence of Mg^{2+} and SO_4^{2-}, on $CaCO_3$ fouling induction period.

Although there were so many studies performed on fouling process, a few of those focused on seawater fouling. With the rapid development of seawater thermal desalination technology, the researches on seawater fouling were not enough to be used as a direct guidance for the design and operation of desalination plants. Seawater fouling process under actual operating conditions should be paid more attention. An experimental study is carried out on seawater fouling process during falling film evaporation according to actual industrial operating conditions in this paper. The results given out could help to set up a complete guidance for engineering design and practical operation of seawater thermal desalination plants.

2. Experimental system

The experimental system is shown in Fig. 1. The working fluid used is Dalian local seawater with the concentration of 3.5%. The tube material is aluminum alloy. The experiment is performed under the atmospheric pressure. Seawater is preheated in a heating tank to the required temperature by an electric heater, and then is transmitted to an upper tank

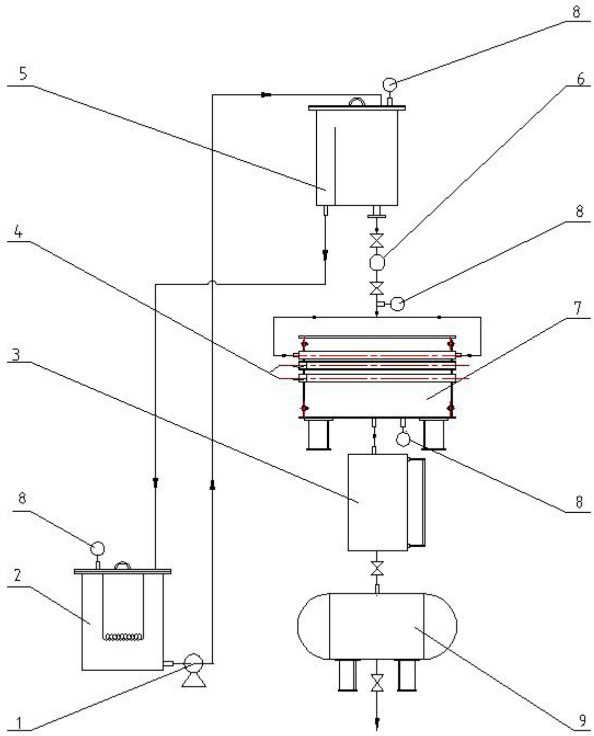

Fig. 1. Diagram of experimental system: 1, Pump; 2, heating tank; 3, measuring tank; 4, electrical heater; 5, upper tank; 6, flow meter; 7, evaporator; 8, thermocouples; and 9, storage tank.

by a pump. An overflow plate is arranged in the upper tank which helps to maintain the stable level of seawater surface. The overflowing water returns to the heating tank for recycling. Through a flow meter, seawater flows from the upper tank into a spray pipe inside the falling film evaporator, and then sprays on the outside of the horizontal heating tubes. After being evaporated, the concentrated brine flows into a measuring tank and a storage tank in turn, and then it is drained off. The scale mass (ΔM) is recorded through weighing the mass of the dried heating tube by an electric balance (with an accuracy of 0.01 mg) at different time. The feed seawater temperature, the spray seawater temperature and the tube surface temperature are measured by thermocouples. The salinity of seawater is measured by a salinometer.

3. Results and analysis

3.1. Growing curves of scale

The seawater concentrations are 3.5% and 7%. The spray densities (Γ) are 0.03, 0.06 and 0.08 kg/(m•s) respectively. The tube surface temperatures (t) are 50°C, 53°C, 60°C, 63°C, 70°C and 73°C, respectively. The experimental results are shown in Figs. 2–5.

Figs. 2–4 present scale growing curves under different tube surface temperatures and spray densities with the seawater concentration of 3.5%. It is concluded that scale mass with the tube surface temperature of 73°C is the biggest and the second big one is with the tube surface temperature of 70°C. For the tube surface temperatures of 63°C and 60°C, the scale masses are very close. For the tube surface temperatures

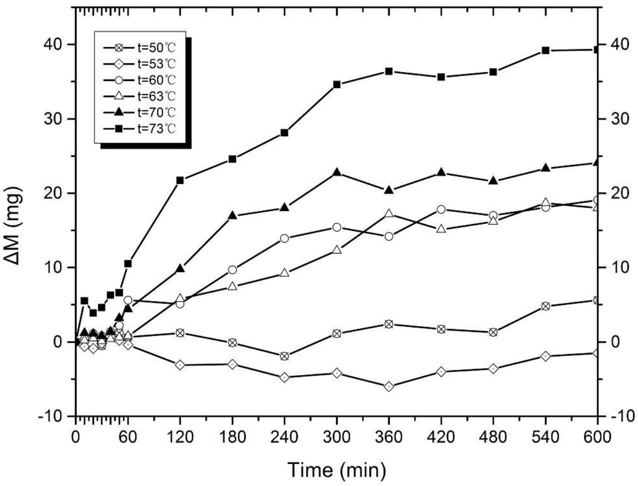

Fig. 2. The growing curves of scale under different tube surface temperatures with the spray density of 0.03 kg/(m•s) and the seawater concentration of 3.5%.

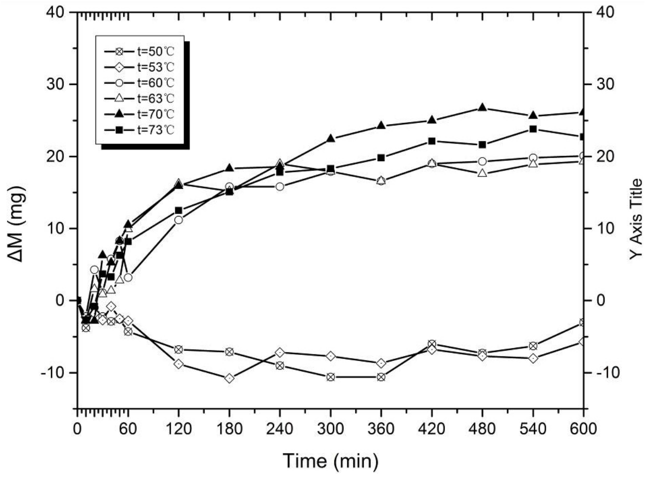

Fig. 4. The growing curves of scale under different tube surface temperatures with the spray density of 0.08 kg/(m•s) and the seawater concentration of 3.5%.

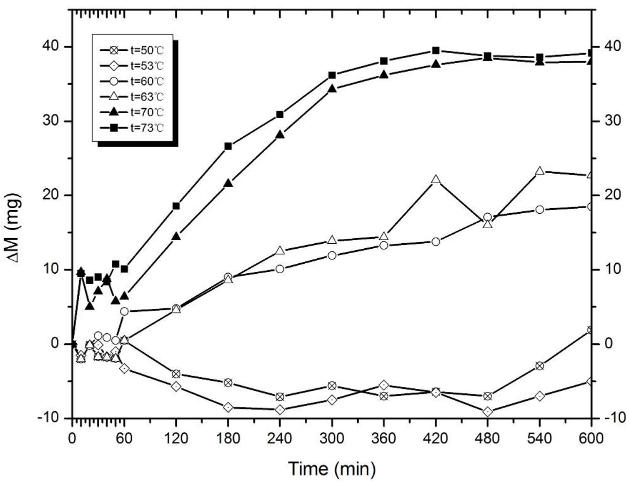

Fig. 3. The growing curves of scale under different tube surface temperatures with the spray density of 0.06 kg/(m•s) and the seawater concentration of 3.5%.

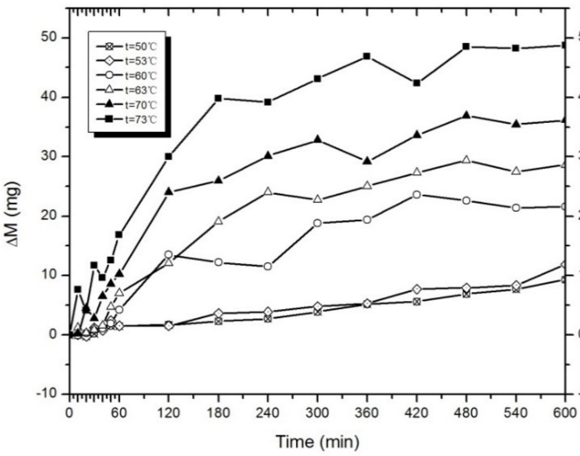

Fig. 5. The growing curves of scale under different tube surface temperatures with the spray density of 0.03 kg/(m•s) and the seawater concentration of 7%.

of 53°C and 50°C, the scale masses are a bit lower than zero, which presents the erosion rate is a bit higher than the scale deposition rate.

Fig. 5 presents the scale growing curves under the spray density of 0.03 kg/(m•s) and the seawater concentration of 7%. It is given out that scale mass increases with the tube surface temperature. For the tube surface temperatures of 53°C and 50°C, vary with that of the seawater concentration of 3.5%, the scale mass is slightly over zero, which presents that the erosion rate is smaller than the scale deposition rate. This is because the scale deposition rate increases greatly with the seawater concentration.

3.2. Scale layer analysis

Effects of the spray density on structure, composition and morphology of scale layer are investigated by an SEM and an energy dispersive X-ray spectroscopy (EDXS). Figs. 6–8 show the scale structures with the magnification times of 300, 500, 1,000 and 5,000 under the spray density of 0.06 kg/(m•s), the seawater concentration of 3.5% and the tube surface temperatures of 50°C, 60°C and 70°C. The X-ray fluorescence is used to test the percentage of Ca and Mg in scale layer.

It can be seen from Figs. 6–9, when the tube surface temperature is 50°C, there presents some scale particles on the tube surface and part of those form into big scale aggregations. With an EDXS, the main component of scale is $CaCO_3$ and the content of which is much higher than that of $Mg(OH)_2$. When the tube surface temperature is 60°C, there are bigger scale particles on the tube surface and the main component of scale is also $CaCO_3$. But the content of $Mg(OH)_2$ is greater than that with the tube surface temperature of 50°C. When the tube surface temperature is 70°C, there are much more scale particles on the tube surface and part of those form into bigger clumps. The content of $Mg(OH)_2$ is greater than the

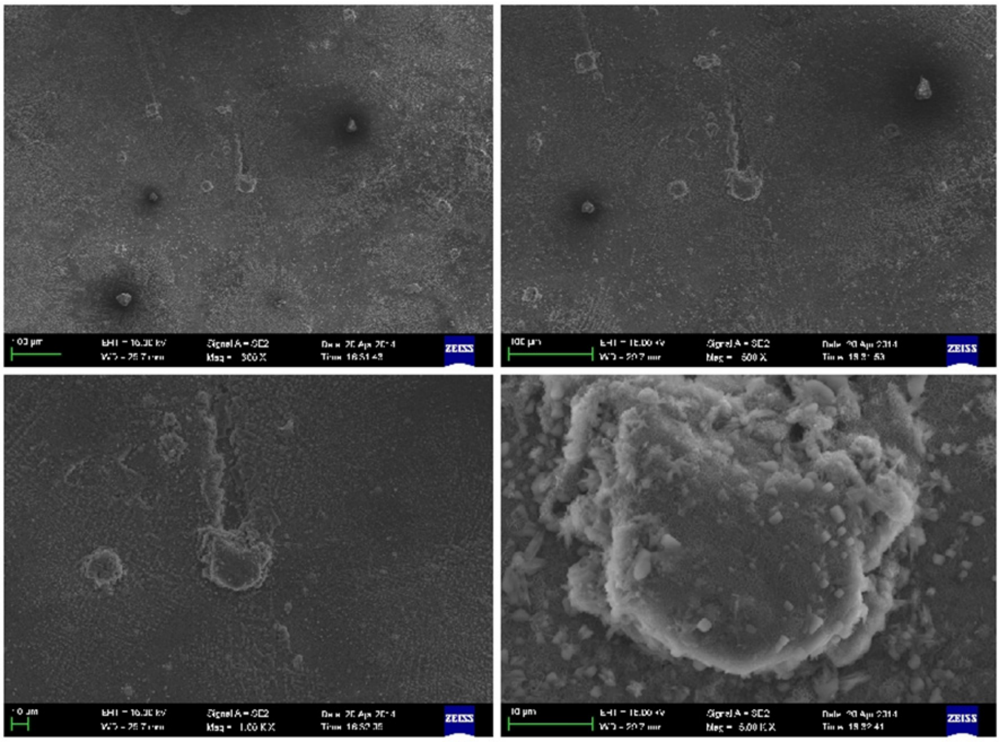

Fig. 6. The SEM images under the tube surface temperature of 50°C, the seawater concentration of 3.5%, and the spray density of 0.06 kg/(m•s), 10 h running.

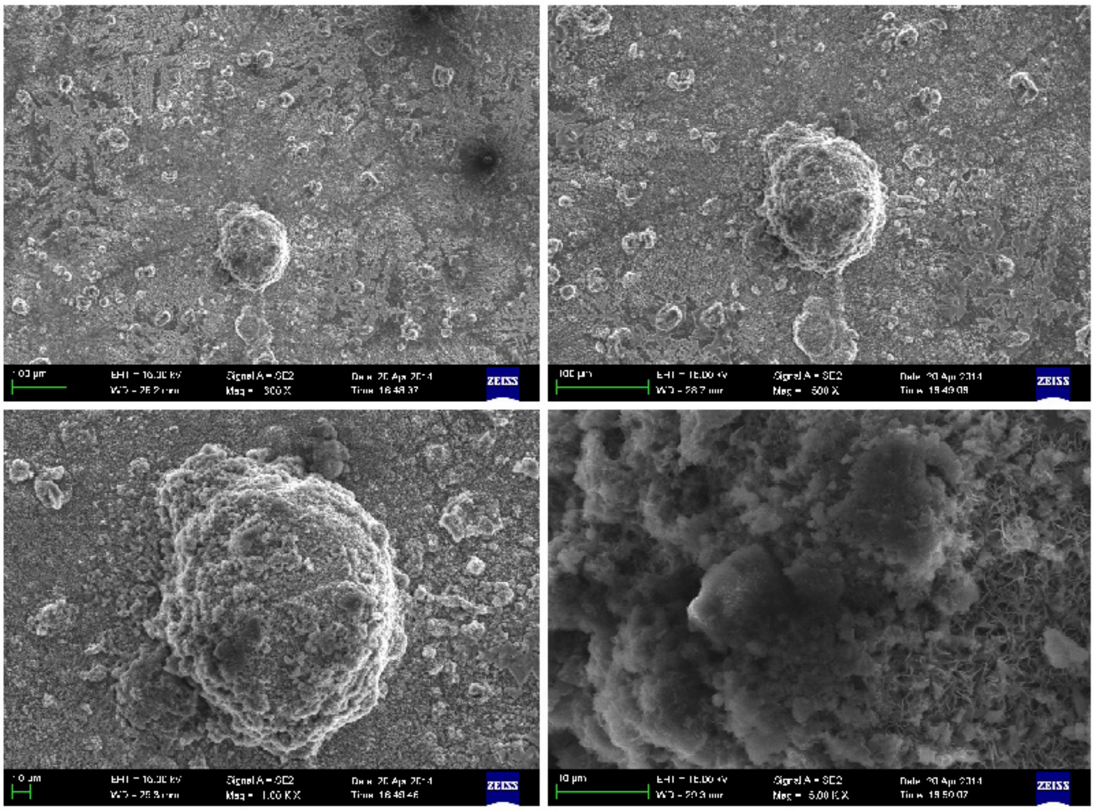

Fig. 7. The SEM images under the tube surface temperature of 60°C, the seawater concentration of 3.5%, and the spray density of 0.06 kg/(m•s), 10 h running.

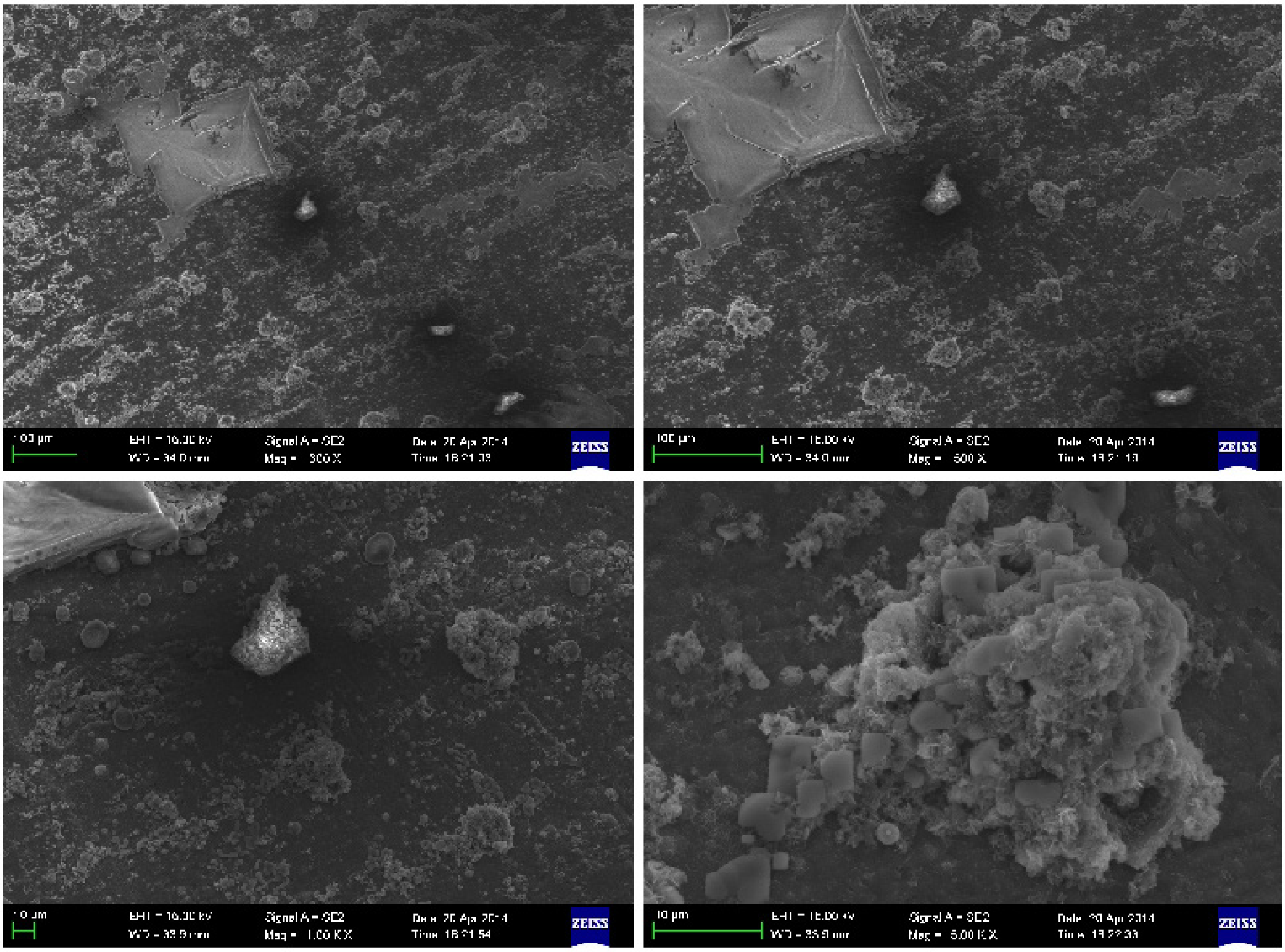

Fig. 8. The SEM images under the tube surface temperature of 70°C, the seawater concentration of 3.5%, and the spray density of 0.06 kg/(m•s), 10 h running.

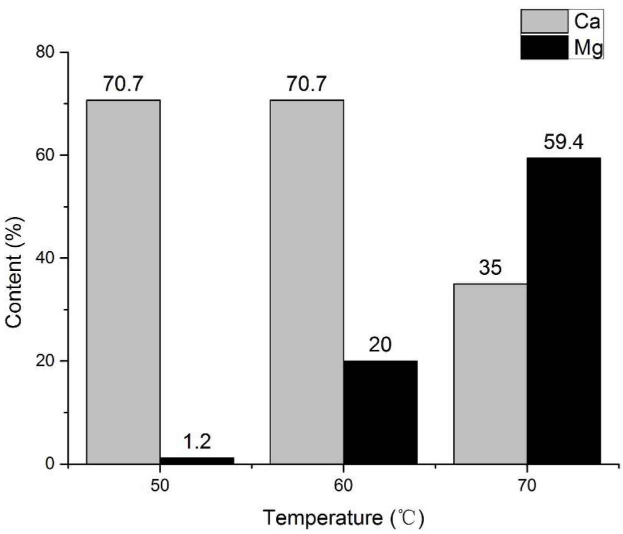

Fig. 9. The calcium and magnesium percentages in scale layer under the seawater concentration of 3.5%, the spray density of 0.06 kg/(m•s), and the tube surface temperatures of 50°C, 60°C and 70°C.

content of $CaCO_3$ and greater than that with the tube surface temperatures of 50°C and 60°C. The content of $CaCO_3$ is smaller than that with the tube surface temperatures of 50°C and 60°C.

4. Conclusions

Dalian local seawater is used as the working agent. The scale growing curves under different conditions are obtained through weighting the scale mass at different time during fouling processes. The morphology and composition of scale layers with different tube surface temperatures are analyzed through an SEM and an EDXS. The results are concluded as follows:

- For the seawater concentration of 3.5%, the erosion rate is higher than the scale deposition rate. For the seawater concentration of 7%, the erosion rate is smaller than the scale deposition rate. The deposition rate of scale increases greatly with the seawater concentration.
- The content of Mg is greater than the content that of Ca for the tube surface temperature of 70°C, but it is opposite for the tube surface temperatures of 50°C and 60°C.

The content of Mg with surface temperature 70°C increases with the tube surface temperature. For the tube surface temperature of 70°C, the content of Ca with surface temperature 70°C is smaller than that with for the tube surface temperatures of 50°C and 60°C.

Acknowledgments

This work is supported by the National Natural Science Foundation of China (No. 51476017), the National Natural Science Foundation of China (No. 51476016), the Natural Science Foundation of Liaoning Province of China (No. 2014020006) and the Key Program of National Natural Science Foundation of China (No.51336001).

References

[1] X.S. Mu, Y. Yang, S.Q. Shen, Experimental research of horizontal tube falling film evaporation in desalination, J. Therm. Sci. Technol., 4 (2011) 291–296.
[2] D. Kern, R.A. Seaton, Theoretical analysis of thermal surface fouling, Br. Chem. Eng., 5 (1959) 258–262.
[3] H.X. Li, Numerical study of fouling deposition on heat transfer surface based on von Carmen analogy, ZJU UD, 4 (2012) 49–50.
[4] Z.M. Xu, J.G. Wang, S.R. Yang, Study on erosion mechanism of particulate fouling, J. Eng. Thermophys., 5 (1998) 611–615.
[5] J. Cleaver, B. Yates, A sub layer model for the deposition of particles from a turbulent flow, Chem. Eng. Sci., 30 (1975) 983–992.
[6] S. Chan, K. Ghassemi, Analytical modeling of calcium carbonate deposition for laminar falling films and turbulent flow in annuli: part 2 – multispecies, J. Heat Transfer, 113 (1991) 741–746.
[7] D. Hasson, H. Sherman, M. Biton, Prediction of Calcium Carbonate Scaling Rates, Proc. 6th International Symposium on Fresh Water from the Sea, Vol. 5, 1978, pp. 193–199.
[8] R. Wang, X.J. Yang, S.H. Lin, Theoretical prediction of $CaCO_3$ scaling rate of circulating water system, Acta Petrol. Sin., 18 (2002) 72–77.
[9] B.Q. Zhang, Y. Li, Z.M. Xu, Experimental study on influencing factors of $CaCO_3$ crystallization fouling process, J. Northeast Dianli. Univ., 28 (2008) 49–54.
[10] L. Zhao, Experimental study of the external conditions on crystallization of calcium carbonate fouling, SDU UD, 5 (2010) 45–46.
[11] Y.D. Liu, Influence of behavior of metallic heat transfer surface on formation characteristics of crystalline fouling, SDU UD, 6 (2011) 75–77.
[12] C.F. Yang, X.D. Xu, Z.Q. Shen, Theoretical analysis and experimental study on $CaCO_3$ scaling induction period, J. Chem. Eng., 45 (1994) 199–205.
[13] T.Q. Liu, X.H. Wang, Fouling induction period of $CaCO_3$ on heated surface, J. Dalian Univ. Technol., 39 (1999) 400–404.
[14] Q.F. Yang, A.Z. Gu, J. Ding, Calcium carbonate fouling behavior and morphology, J. Chem. Eng., 53 (2002) 924–930.
[15] Z.B. Qiu, J.W. Zhang, Z.M. Xu, Experimental investigation and theoretical analysis on the effect of surface energy upon the fouling induction period, J. Northeast Dianli. Univ., 28 (2008) 45–48.
[16] H.W. Li, H.J. Li, P.F. Liu, Fouling induction period of $CaCO_3$ and its influence factors, Fault-Block Oil Gas, 16 (2009) 111–113.